Interspecies bacterial competition determines community assembly in the *C. elegans* intestine

Anthony Ortiz Lopez[1,2,3], Nicole M. Vega[2,*,+] , Jeff Gore[1,2,+]

[1]Microbiology Graduate Program, Massachusetts Institute of Technology, Cambridge, MA, 02139, USA

[2]Physics of Living Systems, Department of Physics, Massachusetts Institute of Technology, Cambridge, MA, 02139, USA

[3]Undergraduate Program on Genomic Sciences, National Autonomous University of Mexico, Cuernavaca, Morelos, 62210, Mexico

*Current address: Department of Biology, Emory University, Atlanta, GA, 30322, USA

[+]Corresponding authors: nvega@emory.edu, gore@mit.edu

Abstract

From insects to mammals, a large variety of animals hold in their intestines complex bacterial communities that play an important role in health and disease. However, the complexity of these gut microbiomes and their hosts often constrains our ability to understand how these bacterial communities assemble and function. In order to elucidate basic principles of community assembly in a host intestine, we study the assembly of the microbiome of *Caenorhabditis elegans* with a bottom-up approach. We colonize the gut of the worm *C. elegans* with 11 bacterial species individually, in all possible pairs, and in selected trios, and we find an organized mixture of coexistence and competitive exclusion that indicates a hierarchical structure in the bacterial interactions. The capacity of a bacterial species fed in monoculture to colonize the *C. elegans* intestine correlates with its average fraction in co-culture experiments, yet fails to predict its abundance in many two- and three-species microbiomes. Hence, the bacterial fractional abundances in co-culture experiments—pairwise outcomes—are influenced by interspecies interactions. These pairwise outcomes accurately predict the trio outcomes in the worm intestine, further highlighting the importance of pairwise interactions in determining community composition. We also find that the *C. elegans* gut environment influences the outcome of co-culture experiments, and demonstrate that the low intestinal pH is one of the causes. These results highlight that a bottom-up approach to microbiome community assembly may provide valuable insight into the structure and composition of complex microbial communities.

Introduction

Bacterial communities are found almost everywhere in nature. Among the many ecosystems in which bacterial communities play a fundamental role, the animal digestive tract is one of remarkable importance. These large, complex, and highly organized consortia can

25 degrade food and deliver nutrients to their host, protect against invading pathogens, and even
26 produce neurotransmitters that affect host behavior (1–7).

27 Despite considerable recent efforts toward elucidating the contents of these bacterial
28 communities (8–11), the rules that govern their assembly are still poorly understood.
29 Complicating this problem is the fact that these microbial communities are exceedingly complex
30 and difficult to manipulate experimentally. The human gut microbiome, for instance, consists of
31 approximately $4x10^{13}$ cells distributed across hundreds of species interacting in myriad ways
32 across different regions of the gut (12). Moreover, these complex microbial communities vary
33 between individuals based on many factors, including environmental conditions, diet, and the
34 host genotype and immune system (13,14). This complexity and variability has stymied efforts
35 to uncover general rules for microbial community assembly in the context of the host
36 environment.

37 Current efforts have taken advantage of model systems to experimentally address the
38 composition and assembly of simpler gut microbiomes (15,16). Animals such as zebrafish (17–
39 19), honey bees (20–23), leeches (24–27), flies (28–31), and worms (32–35) can be raised and
40 manipulated in the laboratory in order to assess their microbiomes. The bacterial communities
41 associated with these animals contain a small number of taxa relative to humans, allowing
42 bottom-up assembly of comprehensive, synthetic microbial communities. These experimentally
43 tractable models provide an opportunity to observe population dynamics in host-associated
44 microbiomes, by exposing a selected population of hosts to colonization under controlled
45 conditions and monitoring the ensuing interactions among microbes and between microbes and
46 host.

47 Here we use the nematode *Caenorhabditis elegans* (36) as a simple gut model to
48 address issues of experimental tractability and to gain intuition about community assembly in

49 microbiomes. Despite comprising only 20 epithelial cells, the *C. elegans* intestinal tract shares
50 many physiological features with the intestines of higher organisms, including microvilli, a mucin
51 layer, epithelial junctions, cyclical movement via contraction of muscles, and extensive
52 interaction with the host immune system (37–43). The gut of *C. elegans* is well known to host
53 stable populations of bacteria, including important pathogens and probiotics of humans, at
54 substantial population levels up to 10^5 bacterial cells per worm (34,44–46). Furthermore, recent
55 reports have suggested that the gut of this millimetric organism is capable of filtering its bacterial
56 environment and selecting a core microbiota (35).

57 In this study, we colonized the intestine of *C. elegans* with simple microbiomes to
58 determine patterns in the assembly of microbial communities in a host intestine. We found that
59 the inherent ability of a bacterial species to colonize the worm gut was an acceptable predictor
60 of that strain's average performance in two-species microbiomes, but these single-species data
61 became inadequate at predicting the outcomes of specific two- and three-species communities.
62 This suggests that interactions between bacterial species determine the shape and form of the
63 microbial communities in this host. Importantly, we find that the outcome of two-species feeding
64 experiments can be used to predict the composition of the three-species feeding experiments,
65 indicating that "assembly rules" may provide insight into the composition of microbiome
66 communities. Further, we identified a conserved bacterial competitive hierarchy between *in vivo*
67 gut and *in vitro* liquid medium that is disabled in specific cases by the acidity of the *C. elegans*
68 intestine. With this, we advance our understanding of the environmental filtering imposed by *C.*
69 *elegans* and provide insight into bacterial community assembly.

70 ## Results

71 To investigate the colonization and growth dynamics of different bacterial species in the
72 gut of *C. elegans*, we fed germ-free synchronized adult worms with eleven single bacterial

73 species over four days in a well-mixed liquid medium (Fig 1A, Methods). This length of feeding
74 was long enough to ensure reliable colonization of the worms, yet short enough to avoid
75 problems associated with pathogen-based killing by our strains (47). After this feeding and
76 colonization period, we allowed worms to feed briefly on heat-killed bacteria to remove transient
77 colonizers, cleaned the surface of the worms, and measured the intestinal bacterial densities by
78 grinding batches of worms and counting colony forming units (CFU, hereafter called *cells*).

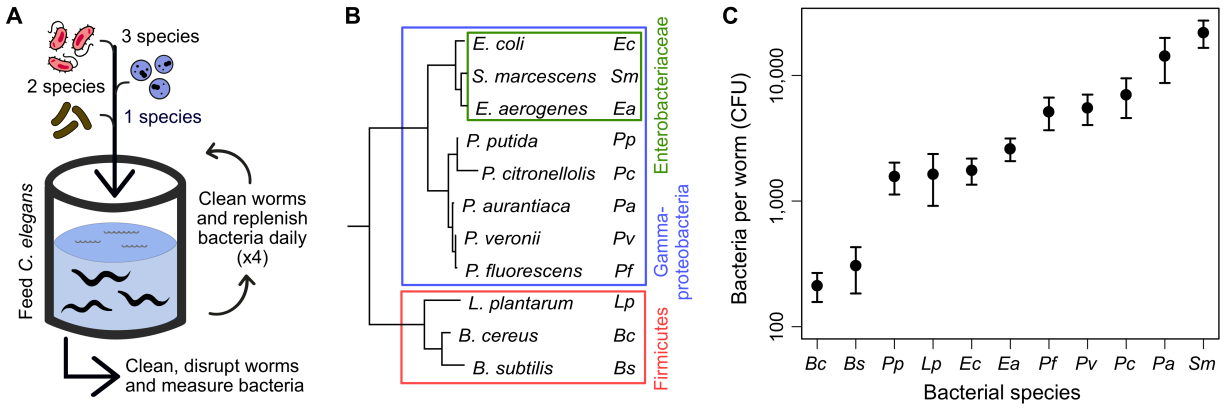

79

80 **Figure 1. Eleven bacterial species colonize the gut of the worm in monoculture. (A)** One,
81 two or three bacterial species are fed in liquid culture to a sterile population of *C. elegans* AU37.
82 Equal bacterial concentrations are maintained during 4 days of colonization. Afterwards, worms
83 are mechanically disrupted in batches of ~20 and CFU counts are used to determine bacterial
84 population sizes. **(B)** Phylogeny of the 11 bacterial species used to colonize the gut of *C.*
85 *elegans*. **(C)** Population sizes in monoculture colonization span two orders of magnitude and
86 reflect the inherent capabilities of bacteria to colonize the worm intestine environment. Points
87 represent the average of 8 or more biological replicates, and error bars as the standard error of
88 the mean (SEM).

89 We utilized a set of eleven bacterial species representing the phyla Firmicutes (gram-
90 positive) and Proteobacteria (gram-negative) (Fig 1B). From the latter phylum, we included soil
91 isolates from the families *Enterobacteriaceae* and *Pseudomonadaceae*, abundant bacterial

clades found in the core microbiota of *C. elegans* grown on its native environment of decaying organic matter (46,48,49), but none of our strains was directly isolated from nematodes. These experiments can therefore be viewed as probing community assembly of a gut microbiome with bacterial species encountered in the natural environment and without a period of evolutionary adaptation. We found that all bacterial species successfully colonized the *C. elegans* intestine, with population sizes ranging from two hundred cells per worm in the case of *Bacillus cereus* (*Bc*), up to tens of thousands of cells in the case of *Serratia marcescens* (*Sm*) (Fig 1C). These differences in bacterial population sizes in monoculture colonization reflect differences in the ability of each bacterial species to not trigger an aversive olfactory response in *C. elegans* (50–52), survive passage through the *C. elegans* grinder (53–56), adhere to the intestinal lumen (32,57–59), proliferate within the worm, or a combination of these features (60).

Despite the importance of revealing which of these characteristics allows each bacterial species to surpass the environmental filtering of the worm gut and reach a given population size, in this study we aimed to understand the influence of monoculture colonization in the assembly of the *C. elegans* microbiome. Thus we constructed the simplest intestinal communities by performing all possible co-culture experiments with these eleven bacterial strains (55 pairs in total). We fed worms in a well-mixed liquid medium with pairs of bacteria present at equal concentrations (*cells*/mL) to ensure that strains had the same initial probability to be ingested (Methods). We found that a majority (41/55~75%) of pairs displayed coexistence of the two species (Fig 2A, left panels), whereas the remainder (14/55) led to competitive exclusion of a species (Fig 2B). Given that we are feeding the worms at equal concentrations, we cannot detect the possibility of bistability, in which the outcome of competition depends upon the starting ratio of the two species. Some bacterial species consistently exclude other species (*Sm*) or are excluded (*Bs*), but the large amount of coexistence (Fig S1) makes the simple winner/loser classification inappropriate for the observed bacterial competitive abilities.

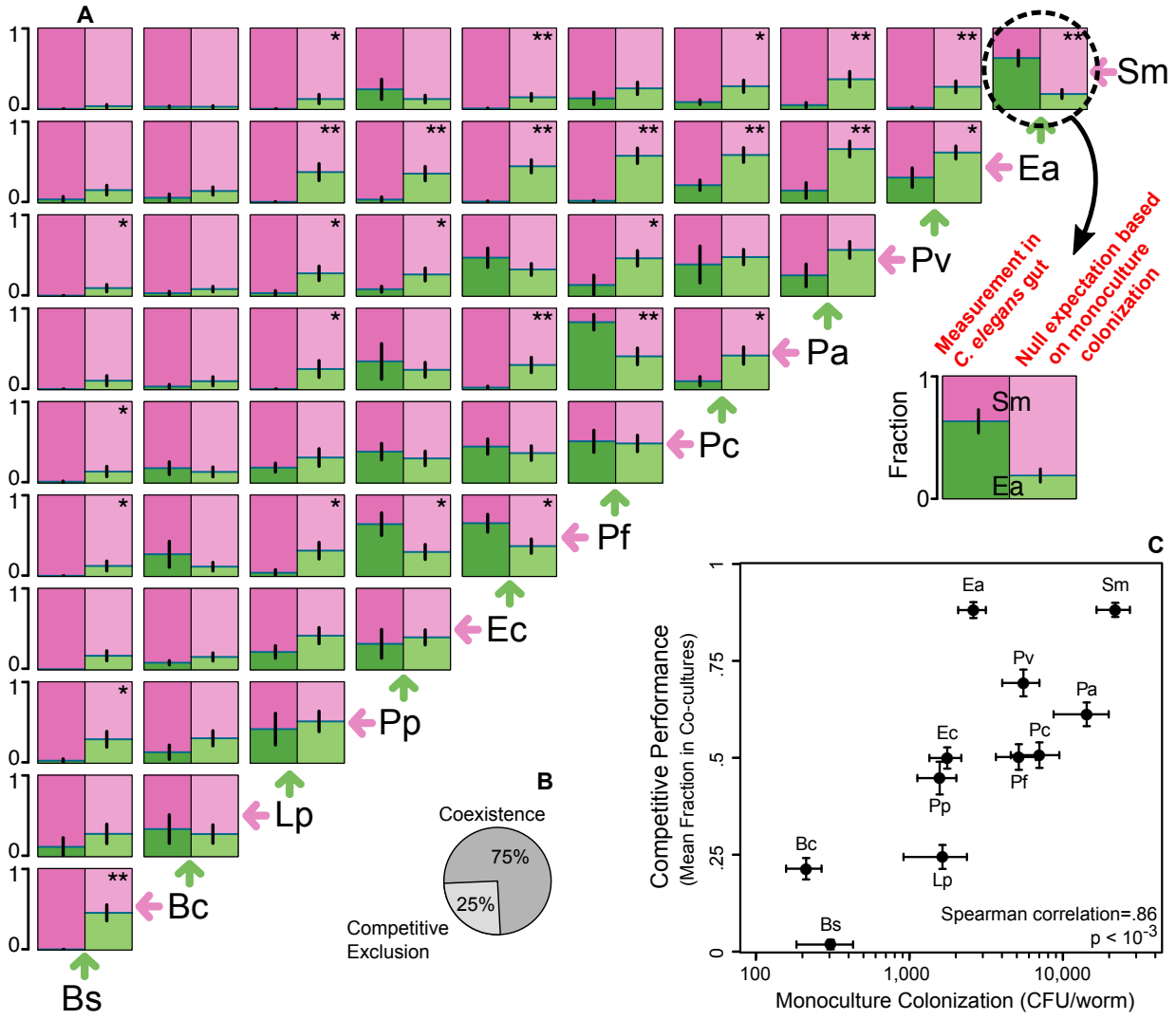

Figure 2. Monoculture colonization relates to, but does not predict pairwise outcomes in the worm intestine. (A) Left: Fractional abundances of 55 co-culture experiments inside the *C. elegans* intestine. Error bars as the SEM of 2 to 8 biological replicates (Fig S1). Bacterial strains are ordered by its mean fractional abundance. **Right:** Null expectation for the fractional abundances based on a non-interacting model where each bacterial species reaches its monoculture population size. Null expectation as the mean of all possible pairings of monoculture information, and error bars as the SEM (Methods). * and ** represent a statistically significant difference between measurement and null expectation at *p*-values of .05 and .01, respectively (Welch's T-test). **(B)** Coexistence is common and competitive exclusion at a

127 detection limit of 2% is rare. **(C)** Competitive performance, as the mean fractional abundance in
128 co-culture experiments, correlates with monoculture population size. X-axis as in Fig 1B, and
129 error bars on Y-axis as the propagated error from the SEM of each pairwise competition.

130 A better summary-metric of the pairwise outcomes is the mean fractional abundance of a
131 species when competed against each of all the other species. Full dominance, extinction, and
132 coexistence award 1 point, 0 points, and the fraction of point at which the species is present in
133 each co-culture experiment, respectively, and the sum is then divided by the number of
134 competitors. We found that this competitive performance score correlates to the population size
135 reached in monoculture colonization (Fig 2C, Spearman correlation $[r_s]$=.86, $p<10^{-3}$). This
136 positive relationship indicates that a bacterial species persists in two-species microbiomes due
137 to similar properties to those favoring its monoculture colonization of the gut. Interestingly, the
138 population sizes do not correlate to the mean relative yields (*cells*/worm of a species in
139 competition divided by *cells*/worm of the same species in monoculture), indicating that a large
140 population size does not protect a bacterial species from being harmed by competition in co-
141 culture experiments (Fig S2).

142 The interactions we measured can be categorized as hierarchical, since a highly ranked
143 competitor will frequently exclude or dominate a low-rank adversary (dominance of pink-color in
144 left panels of Fig 2A). The hierarchy score of this network, 0.82, is significantly larger than the
145 hierarchy score found in random matrices with the same distribution of pairwise outcomes (p
146 $<10^{-5}$, Methods), suggesting that the hierarchy seen in our experiments is caused by bacterial
147 features acting in a transitive manner. Consistent with this, we do not observe any cases of
148 intransitive competition, in which the pairwise interactions of three bacterial species would be
149 analogous to the rock-paper-scissors game and no absolute winner would exist (61,62). This
150 intransitivity has been proposed as a major mechanism inducing coexistence in natural
151 populations (63–67), but we do not observe it in any of our 165 possible trios. With a more

relaxed definition of non-transitivity, in which a species wins a competition by being more abundant than the competitor instead of needing to fully exclude it, we find two candidate trios with a rock-paper-scissors-like structure: *Ec-Pf-Pa* and *Pp-Pf-Pa* (although the dominance of some competitors is not statistically significant).

Lp, *Bs*, and *Bc*, the three species representing the Firmicutes phylum, were competitively excluded in most co-culture experiments, consistent with their poor colonization in monoculture. Likewise, the strongest single species colonizer, *Sm*, dominates the final population in most of its pairwise competitions. However, not all strains and interactions acted according to expectations from single species colonization (68–70). For example, even though its monoculture population size was just above average, *Enterobacter aerogenes* (*Ea*) was capable of outcompeting most of its adversaries, suggesting that direct interactions between microbial species can play a significant role in determining the outcome of pairwise colonization.

We therefore sought to determine whether interactions between microbes are an important determinant of community structure, or whether monoculture colonization ability is sufficient to predict the outcomes of pairwise competition in the host. We calculated a null expectation for the fractional abundances assuming that each species is able to reach the carrying capacity that was measured in monoculture colonization (Fig 2A, right panels). By comparing this null expectation with the experimentally measured fractions obtained from pairwise colonization (Fig 2A, left panels), we are able to identify the cases in which interspecies interactions play a dominant role in determining the composition of the gut microbiome. Across all pairs, the measured fractions deviate from the null expectations by a mean distance of .2, with a peak at low distance and a long tail corresponding to cases where the interspecies interactions are particularly important (Fig S3). In 28 cases this deviation is large enough to reject the null model (p<.05), many more than the 2.75 cases expected by chance at this significance level and with these 55 pairwise combinations. This result indicates that a null

expectation, where each species' abundance in pairwise colonization is largely determined by the initial filtering event rather than by interactions between bacteria, is valid for some but not all pairs of species in this set.

The importance of interspecies interactions is further supported by an analysis of relative yields (Fig S4). Most species cannot reach their monoculture population size in co-culture experiments (relative yield<1), suggesting that interactions between species are largely competitive. The 21 out of 110 cases (19%) where we measured a relative yield larger than one could be due to modest facilitation or due to variation in colonization and measurement between the monoculture and pairwise experiments. Collectively, these data suggest that the monoculture colonization ability of a bacteria relates to its abundance in pairwise experiments, but the mostly competitive interspecies interactions alter as many as half of the individual pairwise outcomes (Fig 2, S4).

Environmental filtering imposed by C. elegans

Next, we sought to characterize the environmental filtering performed by *C. elegans* during microbial community assembly. Specifically, we sought to quantify the differences in bacterial relative abundances between the *in vivo* worm gut and the *in vitro* liquid medium used as feeding substrate (Fig 3). Thus, we performed all fifty five co-culture experiments in liquid medium and measured the equilibrated bacterial fractions after seven cycles of daily dilution (Methods, Fig S5). We found that competitive performance in the worm gut and liquid media are correlated (Fig 3A), which suggests that the environmental filtering that *C. elegans* provides is not strong enough to alter the hierarchical order of these eleven bacterial strains. This resemblance between the worm gut and liquid media with the coarse-grained mean fractional abundance is also observable when comparing the mean relative yields (Fig 3A, inset).

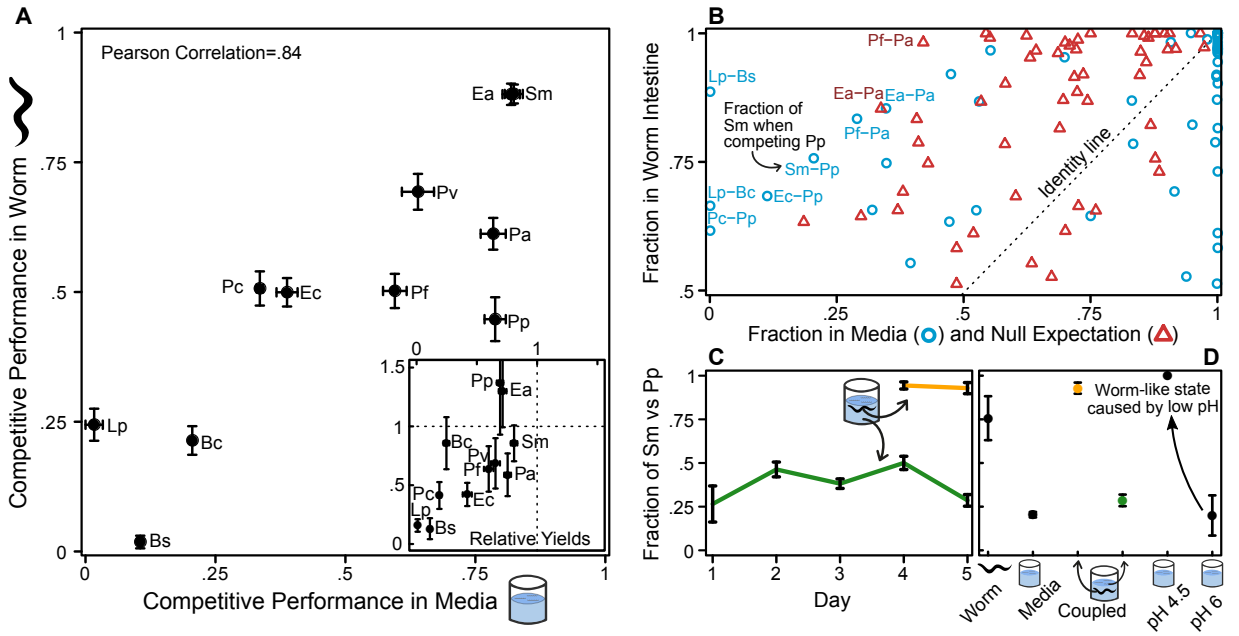

200

201 **Figure 3. Bacterial competitive hierarchy is conserved between *in vivo* gut and *in vitro***
202 **liquid media environments. (A)** Mean fractional abundance in co-culture experiments in the
203 worm and in the background feeding media correlate with each other, indicating that strong
204 competitors remain strong, and weak competitors remain weak in these two environments.
205 **(Inset)** Mean relative yields (*cells*/worm of a species in competition divided by *cells*/worm in
206 monoculture) in the worm and media also correlate. Error bars as the propagated error from the
207 SEM of co-culture experiments. **(B)** Fractional abundances in co-culture experiments in worm
208 intestine are as different from the background media as from the null expectation based on
209 monoculture colonization. Points at distance >.5 from the identity line were labeled. **(C)** Fraction
210 of *Sm* in worm (yellow) and media (green) when environments are coupled by migration. Both
211 environments reach their different equilibrium points in the same test tube. **(D)** An acidic version
212 of the media resembling the average pH of the worm intestine (4.5) shifts back the pairwise
213 outcome of *Sm-Pp* to a worm-like state. Error bars in C and D as the SEM of at least 4
214 replicates.

Although competitive performance is similar between the worm gut and *in vitro* liquid media, we find that individual pairwise outcomes often display very different outcomes in these two environments (Fig 3B). We quantify the competitive performance of a bacterial species by averaging over all ten pairwise experiments; although these averages correlate between the worm intestine and the background media (Fig 3A), the underlying pairwise outcomes can be very different (Fig 3B, blue circles). The mean distance between the fractions in the media and the worm (0.22) is similar to the mean distance between the null expectation from monoculture colonization and the worm outcomes described earlier (Fig 3B, red triangles; Fig S3). If we wanted to predict the relative abundance of two-species communities in the worm intestine, both the monoculture colonization and the media pairwise outcomes would fail to a similar extent, but in dramatically different ways: while the null expectation overestimates the frequency of coexistence in the gut, the media competition displays less coexistence than observed in the worm gut. Our data therefore suggests that the *C. elegans* intestine doesn't alter the competitive hierarchy of its bacterial colonizers, but is capable of shifting specific pairwise outcomes.

In fact, several pairs of species displayed remarkably different outcomes in competition inside versus outside of the worm intestine, such as *Sm-Pp* and *Lp-Bs*. Since the two environments were capable of selecting a different microbial community composition, we wondered if migration between them would homogenize their microbial compositions. To answer this question, we fed again a population of worms with a mixture of *Sm-Pp*, but instead of keeping equal proportions of both species by adding fresh bacteria daily to the batch culture, we allowed the bacteria to be carried over during each dilution step. While the bacterial abundances in the media change and reach equilibrium, at the same time and in the same well, competition takes place within the intestine of worms. Migration between these environments takes place in the form of worms feeding from the media and defecating live bacteria into it. We found that despite the strong linkage between environments, *Sm* dominated in the gut yet was

present in a minority in the media outside the worm (Fig 3C). Similar differences in competition outcomes between the worm gut and outside media were observed for *Lp-Bs* (Fig S6). These results show that the environmental filtering imposed by the worm intestine can be strong enough to keep an internal bacterial community different from its surrounding environment.

Given the importance of pH to microbial growth and competition (71–75), we tested whether the low pH of the worm gut could cause some of the observed differences between competitive outcomes in the intestine and the media. To this end, we repeated the *Sm-Pp* competition in liquid media at its normal pH 6, and at lower pH 4.5, where the latter approximates the conditions within the nematode intestine (76,77). For this pair of species, lowering the pH of the media was sufficient to alter the pairwise outcome, resulting in a community very similar to that observed in the worm intestine (Fig 3D). Similar results were observed in the pair *Lp-Bs* (Fig S6). We conclude that the acidic pH of the worm gut is an important component of the environmental filtering imposed by this host intestine during community assembly.

Trio outcomes are predicted by pairwise outcomes

Our results thus far indicate that monoculture colonization and pairwise interactions are both important for the outcomes of pairwise experiments in the *C. elegans* intestine (Fig 3B). However, it remains unclear how these two forces will impact the assembly of more diverse bacterial communities. We therefore constructed three-species communities to extend our analysis. From our eleven bacterial strains, we purposely selected a set of six (*Bc*, *Lp*, *Pf*, *Pv*, *Ea*, and *Sm*) that covers the different competitive abilities observed. We fed *C. elegans* with the 20 possible three-species combinations of these six species, and measured the bacterial abundances after four days of colonization (Fig S7). To summarize these trio outcomes, we again utilized the mean fractional abundance of each species in all communities where it

264 participates. We found that the population size in monocultures correlates less strongly with this
265 mean fraction in trios (Fig S8, Spearman correlation [r_s]=.6, p=.12) than with the mean fraction
266 in pairwise experiments (Fig 2C). This result indicates that, as community diversity increases,
267 the ability to colonize in monoculture becomes less important.

268 The mean fractional abundance measured in our experiments agrees with previous
269 reports of the natural *C. elegans* microbiota (35), with our *Enterobacteriaceae,*
270 *Pseudomonadaceae*, and Firmicute isolates ranking first, second, and third in abundance,
271 respectively. However, more than confirming the potential that each bacterial species has when
272 competing in a natural setting, our bottom-up approach allows us to examine closely many
273 particular microbiomes. For instance, the trio outcome of *Ea-Pf-Sm* is shown in Figure 4A as a
274 stack of bars, and in Figure 4B as a point in a simplex, where the point moves closer to a vertex
275 when that given species increases in abundance. By plotting the measurements of all 20 trios
276 into one simplex (Fig 4C), we observe that most of the cases have one species as highly
277 abundant, yet full exclusion is rare and only accounts for 3 out of the 20 different communities
278 (Fig 4D).

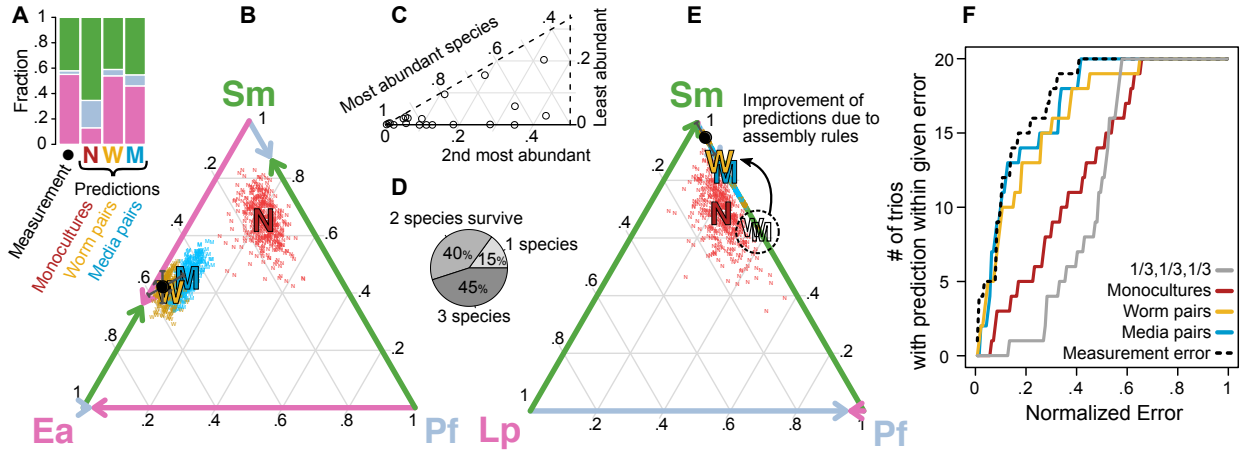

279

280 **Figure 4. Fractional abundances in three-species communities are well predicted by**
281 **pairwise outcomes. (A)** Outcome of trio *Ea-Pf-Sm* in *C. elegans* intestine, together with

predictions based on monocultures (each bacterial species reaches its population size in monoculture) or pairwise outcomes (normalized arithmetic mean) in worm or media. **(B)** Simplex representation of trio outcome and predictions in (A), with the edges depicting the pairwise outcomes in the worm intestine. The error bars on measurement are the SEM of 4 biological replicates, and the clouds of small letters around predictions are 400 bootstrap replicates ('N's sampling the monoculture data, and 'W's and 'M's sampling the pairwise data). **(C)** 20 trio outcomes represented in one 6th of a simplex, with the highest, medium, and lowest abundant species taking the left, right and upper vertices, respectively. **(D)** 3, 8, and 9 out of the 20 trios show full competitive exclusion, two- and three-species coexistence, respectively. **(E)** Assembly rules help the quantitative prediction of the trio outcomes when one of the pairwise outcomes is competitive exclusion. **(F)** Cumulative distribution of error of predictions. Error calculated as the linear distance between prediction and measurement in the simplex. The distances are normalized by the maximal distance, $\sqrt{2}$. The dashed line represents the mean distance between the measured mean and the biological replicates of each trio.

As with the pairwise outcomes, the mean abundance of *Ea* is the least predictable based on its monoculture colonization (Fig S8), which suggests that the pairwise interactions favoring the abundance of *Ea* in co-cultures might favor *Ea* further in larger communities. To determine if pairwise interactions are the main drivers of trio outcomes, we made predictions of all trios based on either monocultures, or pairwise outcomes. To make quantitative predictions of trios based on monocultures, we extended the null expectation described earlier by assuming that all species will reach their monoculture population sizes ('N's in Fig 4 and S7). This null expectation based on monoculture colonization achieves poor results at predicting trio communities, for its mean error of 35.7% is just slightly better than the 43.8% mean error of an uninformed '⅓, ⅓, ⅓' prediction (Fig 4F). Hence, although monoculture colonization predicts pairwise outcomes with a lower mean error of 20% (Fig S3), monocultures become inadequate

307 at predicting three-species microbiomes, highlighting again the importance of interspecies
308 interactions.

309 Alternatively, we can predict trios based on pairwise outcomes by taking the arithmetic
310 mean of each species' abundance in the co-culture experiments against the other two species
311 (here, a normalization factor of 2/3 is needed for the fractions of the three species to add to
312 one). This *normalized arithmetic mean* prediction, applied to the pairwise outcomes obtained in
313 the worm intestine or the *in vitro* liquid media ('W's and 'M's in Fig 4A and B, respectively),
314 quantitatively predicts some trios with high accuracy, and reaches a lower mean error of 26%
315 (Fig S9). However, this simple prediction is prone to error when one of the pairwise outcomes is
316 competitive exclusion, such as *Sm-Lp* in the *Sm-Lp-Pf* trio (Fig 4E, empty letters). Fortunately, a
317 recently proposed 'assembly rule' (69) is capable of adjusting these cases by simply removing a
318 bacterial species from the trio prediction when it cannot survive all pairwise competitions (Fig 4E
319 and S7). After the application of these assembly rules, the mean error of the predictions based
320 on worm or media pairwise outcomes, 18.7 and 15.7%, comes close to the expected biological
321 noise in trio outcomes, 13.3% (Fig 4F). The fact that pairwise outcomes can properly predict trio
322 outcomes indicates that interactions between pairs of bacterial species are an important force in
323 determining the outcome of multispecies communities and suggests that indirect interactions
324 are uncommon or weak.

325 ## Discussion

326 Here we characterized the outcomes of all co-culture experiments among 11 bacterial
327 species within the gut of the worm *C. elegans*. We find that monoculture population size in the
328 worm intestine correlates well with competitive performance in this environment, suggesting that
329 the ability to colonize and proliferate in the host is an important determinant of success.
330 However, we find that the outcomes of pairwise competition, but not single-species colonization

ability alone, predict the outcomes of three-way competition, indicating that pairwise competitive interactions between microbes are an important driver of the assembly of more complex multispecies communities.

We found that most interactions among our set of species are competitive, and none of the 55 pairs that we measured displayed a strong mutualism in which both species benefited. Despite this prevalence of competitive interactions, we also found that coexistence between species was very common, indicating that the competition is relatively weak and only rarely leads to competitive exclusion. Interestingly, we do not observe any cases of strictly non-transitive interactions (rock-paper-scissors) (66) among any of the 165 possible trios, questioning once more the practical significance of this mechanism at stimulating coexistence and diversity in multispecies communities (63). However, the 11 species that we studied here are laboratory isolates rather than a naturally occurring community, which may have evolved to co-occupy their particular environment (78). Such communities could be enriched for mutualistic or rock-paper-scissors interactions; future work will be necessary to determine whether naturally occurring communities have significantly different network properties, although recent work suggests that non-transitive interactions are not common in natural microbial communities (79).

Although we observed a range of different outcomes, from coexistence to competitive exclusion, we have not extensively explored the mechanistic basis behind them. These outcomes could arise from simple resource competition, including competition for the limited space available within the *C. elegans* gut, or there could be more explicit forms of antagonism such as toxin production. In cases of coexistence, spatial partitioning within the host could play an important role; the role of spatial structure was recently found to be important in determining the competitive outcome of interspecies competition within the gut of the zebrafish (17). Further work will be required to elucidate these spatial dynamics within the worm.

355 Our results provide additional support for the importance of host-determined
356 environmental factors, specifically pH, in shaping the microbiome. The low pH of the gut
357 environment is thought to be a critical factor in host-microbe interactions, and recent work has
358 explicitly demonstrated the importance of pH in modulating the interactions between microbes
359 and determining the structure of synthetic and natural communities (71–73). Consistent with
360 these results, we observed that reducing the pH of a liquid medium to simulate the host intestine
361 could alter the outcomes of competition between species and substantially reduce the difference
362 between *in vitro* media and *in vivo* gut.

363 The conserved competitive hierarchy among our set of microbial species inside and
364 outside the worm suggest that similar traits are required for success in both environments.
365 Notably, these experiments were carried out in an immune-deficient host strain (AU37) which is
366 defective in recognition of and response to microbial colonization (80). It remains to be seen
367 whether the more stringent environment of an immune-capable host would produce larger
368 differences between *in vitro* and *in vivo* experiments. In future work, it will therefore be
369 interesting to determine the extent to which modifying the properties of the host environment
370 alters the filtration imposed by that environment and the interactions between colonizing
371 microbial strains.

372 The work presented here focuses on population averages rather than the composition of
373 bacterial communities within individual worms. Recent results from our group have
374 demonstrated that variation between individuals can be informative - when colonization is very
375 slow, there can be an extreme bottleneck during colonization of the worm gut that leads to
376 marked heterogeneity between the gut communities in different worms (81). Similar results have
377 recently been found in *Drosophila* (82), indicating that stochastic effects during colonization may
378 be important in a wide range of host species. Under the feeding densities used in these
379 experiments we expect more uniform colonization, but it will be important for future studies to

380 determine the role of stochasticity and priority effects during assembly of multispecies
381 communities within the host.

382 Our results are based on a single time point after multiple days of colonization, at which
383 point we expect any initial transients in population dynamics to have died out. This experimental
384 choice allows us to focus on community composition after species have had time to interact, but
385 also precludes the study of the early colonization dynamics. *C. elegans* in the wild is born sterile
386 and is then colonized by the complex microbial communities present within the soil and rotting
387 organic matter (83). This is similar to the microbial successions that have been observed in
388 other contexts, such as in the digestive tract of human infants, *in situ* and *in vitro* cheese rind
389 communities, enrichments of seawater in chitin particles, and *in vitro* enrichments of leaf
390 communities (84–87). It would be fascinating to determine whether similar succession dynamics
391 take place during early colonization of the worm intestine.

392 In this study, we have fed worms with monocultures, pairs, and trios of bacteria from a
393 set of naive soil isolates to determine the role of interspecies interactions in the assembly of
394 host-associated microbial communities. These results add to our understanding of how
395 interactions between pairs of bacterial species can inform our understanding of more complex
396 bacterial communities. Our results show the promise of experimental bottom-up microbial
397 ecology as a tool for understanding the dynamics of bacterial gut communities in a simple model
398 organism, providing insight into the forces that shape and control the structure of microbiomes.

399 ## Methods

400 ### *Nematode culture*

401 Nematodes were grown, maintained, and manipulated with standard techniques (88).
402 The *C. elegans* strain AU37 (*glp-4(bn2)* I; *sek-1(km4)* X) was used for all experiments. Due to

403 the *glp-4* mutation, AU37 does not develop gonads and is therefore sterile when raised at room
404 temperature (23-25ºC). Sterility ensured that all worms in a given experiment were of the same
405 age and had the same life history. The mutation on the *sek-1* gene, part of the p38 MAPK
406 signalling pathway (80), decreases immune function and makes AU37 more susceptible to
407 bacterial colonization (41). The ensuing larger intestinal bacterial communities allowed better
408 quantification of fractional abundances. Worm strains were provided by the Caenorhabditis
409 Genetic Center, which is funded by NIH Office of Research Infrastructure Programs (P40
410 OD010440).

411 L1 animals of the same age were obtained using the standard egg-extraction protocol
412 (88). Starved larvae were then transferred to NGM plates with lawns of *E. coli* OP50, and after 2
413 days of feeding at room temperature, a synchronous adult population of *C. elegans* was
414 obtained. Worms were then transferred to S-medium (88) + 100 µg/mL gentamicin + 5X heat-
415 killed OP50 for 24 hours to kill any bacteria inhabiting the intestine, resulting in germ-free
416 worms. Heat-killed OP50 was used to trigger feeding behaviour in the worms. The adult worms
417 were washed via sucrose flotation to remove debris before bacterial colonization.

418 ***Bacteria***

419 *Bacillus subtilis* (ATCC 23857), *Enterobacter aerogenes* (ATCC 13048), *Lactobacillus*
420 *plantarum* (ATCC 8014), *Pseudomonas aurantiaca* (*Pseudomonas chlororaphis* subsp.
421 *aurantiaca*) (ATCC 33663), *Pseudomonas citronellolis* (ATCC 13674), *Pseudomonas*
422 *fluorescens* (ATCC 13525), *Pseudomonas putida* (ATCC 12633), *Pseudomonas veronii* (ATCC
423 700474), *Serratia marcescens* (ATCC 13880) were obtained from ATCC. *Bacillus cereus* was
424 obtained from Ward's Scientific Catalog. *Escherichia coli* MC4100 (CGSC #6152) was obtained
425 from the *E. coli* Genetic Stock Center.

Bacterial strains were grown for 24hrs at 30ºC in individual culture tubes with 2 mL of LB (Difco). To construct cultures to feed *C. elegans*, strains were centrifuged 1 minute at 7K RCF to pellet, washed once in S-medium, and then resuspended in 1% v/v Axenic Medium diluted in S-medium (1%AXN). 100 ml of 100% AXN were prepared by autoclaving 3g yeast extract and 3g soy peptone (Bacto) in 90 ml water, and subsequently adding 1g dextrose, 200µl of 5 mg/ml cholesterol in ethanol, and 10 ml of .5% w/v hemoglobin in 1 mM NaOH. To standardize the bacterial densities used to feed *C. elegans*, the bacterial cultures were diluted to ~10^8 CFU/ml based on previously measured CFU counts.

Bacterial colonization of C. elegans

Germ-free adult worms were resuspended in 1%AXN to a concentration of ~1000 worms/mL. Aliquots of 120µL (~100 worms) were laid into 96-deep-well culture plates (1 mL well volume, Eppendorf). 15µL of each bacterial suspension were added to the corresponding wells in a matrix-like format (11 species x 11 species), leaving a final bacterial concentration of ~2x10^7 CFU/ml, and a 150µl volume for monoculture and co-culture experiments. Extra replicates of monoculture colonization were done to complement the diagonals of the matrices containing the co-culture experiments. For trio competitions, 3 bacterial species were mixed evenly to reach a concentration of ~3x10^7 CFU/ml. Plates were covered with a Breathe-Easy sealing membrane and incubated with shaking at 400 RPM at 25ºC. To maintain the bacterial concentrations constant throughout the 4-day feeding period, every day the worm samples were washed and the bacteria was replenished. Samples were washed with a VIAFLO 96 by adding 500µl of M9 Worm Buffer (WB) + 0.1% v/v Triton X-100 (Tx), pipetting 10 times, and removing the supernatant after worms precipitated. The samples were then transferred to new 96-deep-well plates to leave behind possible biofilms, and then washed in the same way two more times with 1%AXN. Bacterial suspensions from new culture tubes were added as previously described.

Mechanical disruption of worms

The worm samples were washed to remove most external bacteria with the previously described protocol. Samples were then incubated in 100µL S-medium + 2X heat-killed OP50 at 25ºC for one hour to allow the worms to evacuate any non-adhered bacterial cells from the intestine. Worms were then rinsed twice with WB + 0.1%Tx, cooled down 15 min at 4ºC to stop peristalsis, and bleached for 6 minutes at 4ºC with 100µL WB + .2% v/v commercial bleach. Worms were then rinsed three times with cold WB + 0.1%Tx to remove bleach.

For manual disruption, each worm sample was transferred to a small petri dish (6 cm) with 3mL of WB + 1%Tx (the high concentration of surfactant facilitates the upcoming grinding). To guarantee the background media was fully clean, 20µl of the supernatant in each petri dish were collected, serially diluted, and laid in agar plates (see below). Then, a batch of ~20 worms was collected by pipetting 200µl from each petri dish into a 0.5 mL microcentrifuge tube (Kimble Kontes), and the exact number of collected worms was recorded. The volume of each microtube was then reduced to 20µl and the worms were grinded for one minute with a motorized pestle (Kimble Kontes Pellet Pestle, Fisher Scientific). After disruption, tubes were centrifuged two minutes at 7K RCF to collect all material, and the resulting pellet was resuspended in 180µL WB (final volume 200µL) before transfer to 96-well plates for serial dilution in 1X phosphate-buffered saline (PBS).

For 96-deep-well plate disruption, rinsed worms were treated for 20 minutes with 100µL of a solution of SDS + DTT (WB + 0.25% v/v sodium dodecyl sulfate + 3% v/v dithiothreitol [1M, freshly mixed in water], chemicals from Sigma Aldrich) to partially disrupt the cuticle, and then washed twice in WB + 0.1%Tx. A deep-well plate (2 mL square well plate, Axygen) was prepared by adding ~0.2g of a sterile grit (36-mesh silicon carbide, Kramer Industries, autoclaved) to each well. Same as in the manual disruption, the worm samples were transferred

to a small petri dish and supernatant samples were taken. Then, batches of ~20 worms were pipetted into individual wells of the Axygen plate. The plate was covered with parafilm and kept at 4ºC for one hour prior to disruption to reduce heat damage to bacteria. Parafilmed plates were capped with square silicon sealing mats (AxyMat) and disrupted by shaking at high-speed (Retsch MM400, 30 hz for 3 minutes). Plates were then centrifuged at 3K RCF for 2 minutes to collect all material, resuspended by pipetting, and transferred to 96-well plates for serial dilution in PBS.

Measurement of bacterial fractional abundances

The undiluted worm digests and supernatants, together with the serial dilutions 10^{-1}, 10^{-2}, and 10^{-3} of each sample, were plated onto Nutrient Agar (3g yeast extract, 5g peptone, and 15g of agar [Bacto] in one liter of water). The samples were incubated at room temperature for two days to allow distinct colony morphologies to develop. Colonies in all distinguishable dilutions were counted afterwards.

Pairwise and trio outcomes were categorized as coexistence if the rare species was present at an average abundance of more than 2%. This threshold is just above our usual limit of detection of ~1%, which is inversely proportional to the number of colonies counted (~100). The pair *Pf-Ea* (1.7%-98.3%) was defined as coexisting since we could reassure the presence of *Pf* with more than one biological replicate.

Hierarchy scores and generation of random matrices

Utilizing the 11x11 matrix with the fractional abundances in co-culture experiments, the hierarchy score is calculated by: 1) Ordering its rows and columns ascendingly based on the mean fractional abundance; and 2) Taking the mean value of the half-matrix under the diagonal. In a perfectly hierarchical matrix, each competitor will drive to extinction every other species with a lower rank, reaching a hierarchy score of 1. Random matrices were generated to calculate the

499 significance of the observed high hierarchy score. We conserved the distribution of fractional
500 abundances by: 1) Sampling with replacement 55 values of the original matrix; 2) Assigning
501 these random fractional abundances to the lower triangle of a new matrix; and 3) Assigning to
502 the upper triangle of the matrix the values of 1-transpose. For each random matrix generated, a
503 new hierarchy score is calculated as previously described.

504 ***Null expectation of fractional abundances***

505 The null expectation based on monocultures is obtained by averaging the fractional
506 abundances in all possible combinations of monoculture information. Since we have ~10
507 replicates for each species colonizing *C. elegans* in monoculture, the null expectation for the
508 pairwise and trio outcomes is the mean of ~100 and ~1000 different combinations of
509 monoculture data, respectively. The SEM is calculated by dividing the standard deviation of all
510 combinations by sqrt(least number of monoculture replicates). These mean and SEM can also
511 be obtained by bootstrapping (sampling with replacement) the monoculture data.

512 ***Co-culture experiments in vitro***

513 Utilizing the same S-medium + 1%AXN, 96-deep-well culture plates, 150µl volume per
514 sample, and the same matrix format used to colonize *C. elegans*, pairs of bacterial species were
515 mixed at a concentration of 10^5 CFU/ml each. We allowed the bacterial relative abundances' to
516 equilibrate with seven growth-dilution cycles, where the bacteria are diluted 100-fold into fresh
517 media each day. As previously described, we quantified the bacterial abundances by plating into
518 agar.

519 ***Phylogeny reconstruction***

520 Sequences of the full 16S rRNA gene were obtained from NCBI. *Sulfolobus solfataricus*,
521 a thermophilic archaea, was used as an outgroup species to root the tree. Clustal X with default

522 parameters was used to align the sequences (89). PhyML-SMS with default parameters was

523 used to select GTR+G+I as the best model and to infer the tree (90).

524 ## References

525 1. Dethlefsen L, McFall-Ngai M, Relman DA. An ecological and evolutionary perspective on human–microbe
526 mutualism and disease. Nature. 2007;449(7164):811–8.

527 2. Nicholson JK, Holmes E, Kinross J, Burcelin R, Gibson G, Jia W, et al. Host-gut microbiota metabolic
528 interactions. Science. 2012 Jun 8;336(6086):1262–7.

529 3. Bercik P, Denou E, Collins J, Jackson W, Lu J, Jury J, et al. The intestinal microbiota affect central levels of
530 brain-derived neurotropic factor and behavior in mice. Gastroenterology. 2011 Aug;141(2):599–609, 609.e1–3.

531 4. Mark Welch JL, Rossetti BJ, Rieken CW, Dewhirst FE, Borisy GG. Biogeography of a human oral microbiome at
532 the micron scale. Proc Natl Acad Sci U S A. 2016 Feb 9;113(6):E791–800.

533 5. Engel P, Moran NA. The gut microbiota of insects – diversity in structure and function. FEMS Microbiol Rev.
534 2013;37(5):699–735.

535 6. Douglas AE. Fundamentals of Microbiome Science: How Microbes Shape Animal Biology. Princeton University
536 Press; 2018. 248 p.

537 7. McFall-Ngai M, Hadfield MG, Bosch TCG, Carey HV, Domazet-Lošo T, Douglas AE, et al. Animals in a bacterial
538 world, a new imperative for the life sciences. Proceedings of the National Academy of Sciences.
539 2013;110(9):3229–36.

540 8. Human Microbiome Project Consortium. Structure, function and diversity of the healthy human microbiome.
541 Nature. 2012 Jun 13;486(7402):207–14.

542 9. Ellegaard KM, Engel P. Beyond 16S rRNA Community Profiling: Intra-Species Diversity in the Gut Microbiota.
543 Front Microbiol. 2016 Sep 21;7:1475.

544 10. Le Chatelier E, Nielsen T, Qin J, Prifti E, Hildebrand F, Falony G, et al. Richness of human gut microbiome
545 correlates with metabolic markers. Nature. 2013 Aug 29;500(7464):541–6.

546 11. Rodríguez JM, Murphy K, Stanton C, Ross RP, Kober OI, Juge N, et al. The composition of the gut microbiota
547 throughout life, with an emphasis on early life. Microb Ecol Health Dis. 2015 Feb 2;26:26050.

548 12. Sender R, Fuchs S, Milo R. Revised Estimates for the Number of Human and Bacteria Cells in the Body. PLoS
549 Biol. 2016 Aug;14(8):e1002533.

550 13. Ley RE, Peterson DA, Gordon JI. Ecological and evolutionary forces shaping microbial diversity in the human
551 intestine. Cell. 2006 Feb 24;124(4):837–48.

552 14. Kau AL, Ahern PP, Griffin NW, Goodman AL, Gordon JI. Human nutrition, the gut microbiome and the immune
553 system. Nature. 2011;474(7351):327–36.

554 15. Bordenstein SR, Theis KR. Host Biology in Light of the Microbiome: Ten Principles of Holobionts and
555 Hologenomes. PLoS Biol. 2015 Aug;13(8):e1002226.

556 16. Douglas AE. Multiorganismal insects: diversity and function of resident microorganisms. Annu Rev Entomol.
557 2015 Jan 7;60:17–34.

558 17. Jemielita M, Taormina MJ, Burns AR, Hampton JS, Rolig AS, Guillemin K, et al. Spatial and temporal features of
559 the growth of a bacterial species colonizing the zebrafish gut. MBio [Internet]. 2014 Dec 16;5(6). Available from:
560 http://dx.doi.org/10.1128/mBio.01751-14

561 18. Rawls JF, Mahowald MA, Ley RE, Gordon JI. Reciprocal gut microbiota transplants from zebrafish and mice to
562 germ-free recipients reveal host habitat selection. Cell. 2006 Oct 20;127(2):423–33.

563 19. Roeselers G, Mittge EK, Stephens WZ, Parichy DM, Cavanaugh CM, Guillemin K, et al. Evidence for a core gut
564 microbiota in the zebrafish. ISME J. 2011 Oct;5(10):1595–608.

565 20. Kwong WK, Moran NA. Evolution of host specialization in gut microbes: the bee gut as a model. Gut Microbes.

2015;6(3):214–20.

21. Engel P, Kwong WK, McFrederick Q, Anderson KE, Barribeau SM, Chandler JA, et al. The Bee Microbiome: Impact on Bee Health and Model for Evolution and Ecology of Host-Microbe Interactions. MBio. 2016 Apr 26;7(2):e02164–15.
22. Motta EVS, Raymann K, Moran NA. Glyphosate perturbs the gut microbiota of honey bees. Proc Natl Acad Sci U S A. 2018 Oct 9;115(41):10305–10.
23. Raymann K, Moran NA. The role of the gut microbiome in health and disease of adult honey bee workers. Curr Opin Insect Sci. 2018 Apr;26:97–104.
24. Graf J, Kikuchi Y, Rio RVM. Leeches and their microbiota: naturally simple symbiosis models. Trends Microbiol. 2006 Aug;14(8):365–71.
25. Marden JN, McClure EA, Beka L, Graf J. Host Matters: Medicinal Leech Digestive-Tract Symbionts and Their Pathogenic Potential. Front Microbiol. 2016 Oct 13;7:1569.
26. Ott BM, Rickards A, Gehrke L, Rio RVM. Characterization of shed medicinal leech mucus reveals a diverse microbiota. Front Microbiol. 2014;5:757.
27. Maltz MA, Bomar L, Lapierre P, Morrison HG, McClure EA, Sogin ML, et al. Metagenomic analysis of the medicinal leech gut microbiota. Front Microbiol. 2014 Apr 17;5:151.
28. Wong AC-N, Chaston JM, Douglas AE. The inconstant gut microbiota of Drosophila species revealed by 16S rRNA gene analysis. ISME J. 2013;7(10):1922–32.
29. Broderick NA, Buchon N, Lemaitre B. Microbiota-induced changes in drosophila melanogaster host gene expression and gut morphology. MBio. 2014 May 27;5(3):e01117–14.
30. Wong AC-N, -N. Wong AC, Luo Y, Jing X, Franzenburg S, Bost A, et al. The Host as the Driver of the Microbiota in the Gut and External Environment of Drosophila melanogaster. Appl Environ Microbiol. 2015;81(18):6232–40.
31. Newell PD, Douglas AE. Interspecies Interactions Determine the Impact of the Gut Microbiota on Nutrient Allocation in Drosophila melanogaster. Appl Environ Microbiol. 2013;80(2):788–96.
32. Aballay A. Caenorhabditis elegans as a host for the study of host–pathogen interactions. Curr Opin Microbiol. 2002;5(1):97–101.
33. Peleg AY, Tampakakis E, Fuchs BB, Eliopoulos GM, Moellering RC Jr, Mylonakis E. Prokaryote-eukaryote interactions identified by using Caenorhabditis elegans. Proc Natl Acad Sci U S A. 2008 Sep 23;105(38):14585–90.
34. Portal-Celhay C, Blaser MJ. Competition and resilience between founder and introduced bacteria in the Caenorhabditis elegans gut. Infect Immun. 2012 Mar;80(3):1288–99.
35. Zhang F, Berg M, Dierking K, Félix M-A, Shapira M, Samuel BS, et al. Caenorhabditis elegans as a Model for Microbiome Research. Front Microbiol. 2017 Mar 23;8:485.
36. Corsi AK, Wightman B, Chalfie M. A Transparent Window into Biology: A Primer on Caenorhabditis elegans. Genetics. 2015 Jun;200(2):387–407.
37. Cabreiro F, Gems D. Worms need microbes too: microbiota, health and aging in Caenorhabditis elegans. EMBO Mol Med. 2013 Sep;5(9):1300–10.
38. Sim S, Hibberd ML. Caenorhabditis elegans susceptibility to gut Enterococcus faecalis infection is associated with fat metabolism and epithelial junction integrity. BMC Microbiol. 2016 Jan 15;16:6.
39. Balla KM, Troemel ER. Caenorhabditis elegans as a model for intracellular pathogen infection. Cell Microbiol. 2013 Aug;15(8):1313–22.
40. McGhee JD. The Caenorhabditis elegans intestine. Wiley Interdiscip Rev Dev Biol. 2013 May;2(3):347–67.
41. Irazoqui JE, Urbach JM, Ausubel FM. Evolution of host innate defence: insights from Caenorhabditis elegans and primitive invertebrates. Nat Rev Immunol. 2010 Jan;10(1):47–58.
42. Ewbank JJ, Zugasti O. C. elegans: model host and tool for antimicrobial drug discovery. Dis Model Mech. 2011 May;4(3):300–4.
43. Thomas JH. Genetic analysis of defecation in Caenorhabditis elegans. Genetics. 1990 Apr;124(4):855–72.
44. Kurz CL. Virulence factors of the human opportunistic pathogen Serratia marcescens identified by in vivo

614 screening. EMBO J. 2003;22(7):1451–60.

615 45. Aballay A, Yorgey P, Ausubel FM. Salmonella typhimurium proliferates and establishes a persistent infection in
616 the intestine of Caenorhabditis elegans. Curr Biol. 2000 Nov 30;10(23):1539–42.

617 46. Berg M, Stenuit B, Ho J, Wang A, Parke C, Knight M, et al. Assembly of the Caenorhabditis elegans gut
618 microbiota from diverse soil microbial environments. ISME J. 2016 Aug;10(8):1998–2009.

619 47. Penley MJ, Greenberg AB, Khalid A, Namburar SR, Morran LT. No measurable fitness cost to experimentally
620 evolved host defence in the Caenorhabditis elegans-Serratia marcescens host-parasite system. J Evol Biol.
621 2018;31(12):1976–81.

622 48. Samuel BS, Rowedder H, Braendle C, Félix M-A, Ruvkun G. Caenorhabditis elegans responses to bacteria from
623 its natural habitats. Proc Natl Acad Sci U S A. 2016 Jul 5;113(27):E3941–9.

624 49. Dirksen P, Marsh SA, Braker I, Heitland N, Wagner S, Nakad R, et al. The native microbiome of the nematode
625 Caenorhabditis elegans: gateway to a new host-microbiome model. BMC Biol. 2016 May 9;14:38.

626 50. Zhang Y, Lu H, Bargmann CI. Pathogenic bacteria induce aversive olfactory learning in Caenorhabditis elegans.
627 Nature. 2005 Nov 10;438(7065):179–84.

628 51. Shtonda BB, Avery L. Dietary choice behavior in Caenorhabditis elegans. J Exp Biol. 2006 Jan;209(Pt 1):89–
629 102.

630 52. Pradel E, Zhang Y, Pujol N, Matsuyama T, Bargmann CI, Ewbank JJ. Detection and avoidance of a natural
631 product from the pathogenic bacterium Serratia marcescens by Caenorhabditis elegans. Proceedings of the
632 National Academy of Sciences. 2007;104(7):2295–300.

633 53. Albertson DG, Thomson JN. The Pharynx of Caenorhabditis elegans. Philos Trans R Soc Lond B Biol Sci.
634 1976;275(938):299–325.

635 54. Avery L. Food transport in the C. elegans pharynx. J Exp Biol. 2003;206(14):2441–57.

636 55. Fang-Yen C, Avery L, Samuel ADT. Two size-selective mechanisms specifically trap bacteria-sized food
637 particles in Caenorhabditis elegans. Proc Natl Acad Sci U S A. 2009 Nov 24;106(47):20093–6.

638 56. Avery L, You Y-J. C. elegans feeding. WormBook. 2012 May 21;1–23.

639 57. Cremer J, Segota I, Yang C-Y, Arnoldini M, Sauls JT, Zhang Z, et al. Effect of flow and peristaltic mixing on
640 bacterial growth in a gut-like channel. Proceedings of the National Academy of Sciences. 2016;113(41):11414–9.

641 58. Wiles TJ, Jemielita M, Baker RP, Schlomann BH, Logan SL, Ganz J, et al. Host Gut Motility Promotes
642 Competitive Exclusion within a Model Intestinal Microbiota. PLoS Biol. 2016 Jul;14(7):e1002517.

643 59. Hodgkin J, Kuwabara PE, Corneliussen B. A novel bacterial pathogen, Microbacterium nematophilum, induces
644 morphological change in the nematode C. elegans. Curr Biol. 2000;10(24):1615–8.

645 60. Sifri CD, Begun J, Ausubel FM. The worm has turned--microbial virulence modeled in Caenorhabditis elegans.
646 Trends Microbiol. 2005 Mar;13(3):119–27.

647 61. Sinervo B, Lively CM. The rock–paper–scissors game and the evolution of alternative male strategies. Nature.
648 1996;380(6571):240–3.

649 62. Nowak MA. Evolutionary Dynamics. Harvard University Press; 2006. 363 p.

650 63. Soliveres S, Lehmann A, Boch S, Altermatt F, Carrara F, Crowther TW, et al. Intransitive competition is common
651 across five major taxonomic groups and is driven by productivity, competitive rank and functional traits. J Ecol.
652 2018;106(3):852–64.

653 64. Narisawa N, Haruta S, Arai H, Ishii M, Igarashi Y. Coexistence of antibiotic-producing and antibiotic-sensitive
654 bacteria in biofilms is mediated by resistant bacteria. Appl Environ Microbiol. 2008 Jun;74(12):3887–94.

655 65. Hibbing ME, Fuqua C, Parsek MR, Peterson SB. Bacterial competition: surviving and thriving in the microbial
656 jungle. Nat Rev Microbiol. 2010 Jan;8(1):15–25.

657 66. Kerr B, Riley MA, Feldman MW, Bohannan BJM. Local dispersal promotes biodiversity in a real-life game of
658 rock–paper–scissors. Nature. 2002;418(6894):171–4.

659 67. Levine JM, Bascompte J, Adler PB, Allesina S. Beyond pairwise mechanisms of species coexistence in complex
660 communities. Nature. 2017 May 31;546(7656):56–64.

661 68. Concepción-Acevedo J, Weiss HN, Chaudhry WN, Levin BR. Malthusian Parameters as Estimators of the

662 Fitness of Microbes: A Cautionary Tale about the Low Side of High Throughput. PLoS One. 2015 Jun
663 26;10(6):e0126915.

664 69. Friedman J, Higgins LM, Gore J. Community structure follows simple assembly rules in microbial microcosms.
665 Nat Ecol Evol. 2017 Mar 27;1(5):109.

666 70. Wolfe BE. Using Cultivated Microbial Communities To Dissect Microbiome Assembly: Challenges, Limitations,
667 and the Path Ahead. mSystems [Internet]. 2018 Mar;3(2). Available from:
668 http://dx.doi.org/10.1128/mSystems.00161-17

669 71. Ratzke C, Gore J. Modifying and reacting to the environmental pH can drive bacterial interactions. PLoS Biol.
670 2018 Mar;16(3):e2004248.

671 72. Ratzke C, Denk J, Gore J. Ecological suicide in microbes. Nat Ecol Evol. 2018 May;2(5):867–72.

672 73. Ilhan ZE, Marcus AK, Kang D-W, Rittmann BE, Krajmalnik-Brown R. pH-Mediated Microbial and Metabolic
673 Interactions in Fecal Enrichment Cultures. mSphere [Internet]. 2017 May;2(3). Available from:
674 http://dx.doi.org/10.1128/mSphere.00047-17

675 74. Fierer N, Jackson RB. The diversity and biogeography of soil bacterial communities. Proceedings of the National
676 Academy of Sciences. 2006;103(3):626–31.

677 75. Bahram M, Hildebrand F, Forslund SK, Anderson JL, Soudzilovskaia NA, Bodegom PM, et al. Structure and
678 function of the global topsoil microbiome. Nature. 2018 Aug;560(7717):233–7.

679 76. Chauhan VM, Orsi G, Brown A, Pritchard DI, Aylott JW. Mapping the pharyngeal and intestinal pH of
680 Caenorhabditis elegans and real-time luminal pH oscillations using extended dynamic range pH-sensitive
681 nanosensors. ACS Nano. 2013 Jun 25;7(6):5577–87.

682 77. Allman E, Johnson D, Nehrke K. Loss of the apical V-ATPase a-subunit VHA-6 prevents acidification of the
683 intestinal lumen during a rhythmic behavior in C. elegans. Am J Physiol Cell Physiol. 2009 Nov;297(5):C1071–
684 81.

685 78. Foster KR, Bell T. Competition, not cooperation, dominates interactions among culturable microbial species. Curr
686 Biol. 2012 Oct 9;22(19):1845–50.

687 79. Higgins LM, Friedman J, Shen H, Gore J. Co-occurring soil bacteria exhibit a robust competitive hierarchy and
688 lack of non-transitive interactions [Internet]. 2017. Available from: http://dx.doi.org/10.1101/175737

689 80. Kim DH. A Conserved p38 MAP Kinase Pathway in Caenorhabditis elegans Innate Immunity. Science.
690 2002;297(5581):623–6.

691 81. Vega NM, Gore J. Stochastic assembly produces heterogeneous communities in the Caenorhabditis elegans
692 intestine. PLoS Biol. 2017 Mar;15(3):e2000633.

693 82. Obadia B, Güvener ZT, Zhang V, Ceja-Navarro JA, Brodie EL, Ja WW, et al. Probabilistic Invasion Underlies
694 Natural Gut Microbiome Stability. Curr Biol. 2017 Jul 10;27(13):1999–2006.e8.

695 83. Schulenburg H, Félix M-A. The Natural Biotic Environment of Caenorhabditis elegans. Genetics.
696 2017;206(1):55–86.

697 84. Palmer C, Bik EM, DiGiulio DB, Relman DA, Brown PO. Development of the human infant intestinal microbiota.
698 PLoS biology. 2007 Jun 26;5(7):e177.

699 85. Wolfe BE, Button JE, Santarelli M, Dutton RJ. Cheese rind communities provide tractable systems for in situ and
700 in vitro studies of microbial diversity. Cell. 2014 Jul 17;158(2):422–33.

701 86. Datta MS, Sliwerska E, Gore J, Polz MF, Cordero OX. Microbial interactions lead to rapid micro-scale
702 successions on model marine particles. Nat Commun. 2016 Jun 17;7:11965.

703 87.Goldford JE, Lu N, Bajić D, Estrela S, Tikhonov M, Sanchez-Gorostiaga A, Segrè D, Mehta P, Sanchez A.
704 Emergent simplicity in microbial community assembly. Science. 2018 Aug 3;361(6401):469-74.

705 88. Stiernagle T. Maintenance of C. elegans. WormBook. 2006 Feb 11;1–11.

706 89. Larkin MA, Blackshields G, Brown NP, Chenna R, McGettigan PA, McWilliam H, et al. Clustal W and Clustal X
707 version 2.0. Bioinformatics. 2007;23(21):2947–8.

708 90. Lefort V, Longueville J-E, Gascuel O. SMS: Smart Model Selection in PhyML. Mol Biol Evol. 2017 Sep
709 1;34(9):2422–4.

710